


LEGIBILITY NOTICE

A major purpose of the Technical Information Center is to provide the broadest dissemination possible of information contained in DOE's Research and Development Reports to business, industry, the academic community, and federal, state and local governments.

Although a small portion of this report is not reproducible, it is being  made available to expedite the availability of information on the research discussed herein.

CONF

NOTICE

PORTIONS OF THIS REPORT ARE ILLEGIBLE. It has been reproduced from the best available copy to permit the broadest possible availability.

Los Alamos National Laboratory is operated by the University of California for the United States Department of Energy under contract W-7405-ENG-36.

CONF-831265-4

LA-UR--84-1190

TITLE:

DE84 011371

INDUCTIVELY STABILIZED EXCIMER LASERS

DISCLAIMER

AUTHOR(S):

Robert C. Sze

This report was prepared as an account of work sponsored by an agency of the United States Government. Neither the United States Government nor any agency thereof, nor any of their employees, makes any warranty, express or implied, or assumes any legal liability or responsibility for the accuracy, completeness, or usefulness of any information, apparatus, product, or process disclosed, or represents that its use would not infringe privately owned rights. Reference herein to any specific commercial product, process, or service by trade name, trademark, manufacturer, or otherwise does not necessarily constitute or imply its endorsement, recommendation, or favoring by the United States Government or any agency thereof. The views and opinions of authors expressed herein do not necessarily state or reflect those of the United States Government or any agency thereof.

SUBMITTED TO:

Proceedings for the International Conference on Lasers 1983
San Francisco, CA, December 1983

MASTER

By acceptance of this article, the publisher recognizes that the U.S. Government retains a nonexclusive, royalty-free license to publish or reproduce the published form of this contribution, or to allow others to do so, for U.S. Government purposes.

The Los Alamos National Laboratory requests that the publisher identify this article as work performed under the auspices of the U.S. Department of Energy

Los Alamos Los Alamos National Laboratory
Los Alamos, New Mexico 87545

228

INDUCTIVELY STABILIZED EXCIMER LASERS

Robert C. Sze
Los Alamos National Laboratory
P. O. Box 1663
Los Alamos, New Mexico 87545

Introduction

Rare-gas halide avalanche discharges, including some form of preionization of the discharge volume, are known to have a limited stable discharge time. The end of the stable discharge time is characterized by streamer arcs propagating across the electrodes. This time is dependent on the electrode separation, the constituents and pressure of the gas mixture, as well as the electrical excitation characteristics. Thus, in the more conventional commercial lasers the laser outputs are short pulsed (15-30 ns) and discharge techniques are developed to deposit most of the stored electrical energy within the stable discharge time of the device. Lin and Levatter [1] have investigated the regimes in which streamer arc formation can be avoided. Such lasers require very uniform preionization with extremely fast voltage risetimes. The additional incorporation of an electrical prepulse has resulted in very high-efficiency, high-energy large volume discharge rare-gas halide lasers [2].

This paper presents another approach to solving the problem of discharge stability. The development of a segmented electrode structure with each element ballasted by an inductor has resulted in very stable discharges and long pulse length laser outputs. The passive stabilization of the rare-gas halide discharges is attributed mainly to the increase in voltage drop across the inductor of a particular segment of the electrode as the discharge in that region begins to go unstable. The advantage of the technique is that the very fast voltage risetime requirement is no longer essential, and the use of conventional thyatron switches without subsequent pulse sharpening circuits is now possible. Presently only small laser devices have been constructed. The 20-cm active length lasers have produced laser pulse lengths greater than 200 ns with efficiencies as high as 1%. Since the intracavity powers for the long-pulsed, short gain length devices are in the region of 200 kW, an order of magnitude below the saturation powers of rare-gas halide lasers, much improved extraction efficiencies are anticipated for longer gain length devices. The small long pulse lasers find applications in injection-locking large energy short pulsed lasers in the regenerative amplifier mode without worry of jitter between the two devices. XeCl, XeF, KrF short pulse lasers have all been injection-locked in this manner giving high energy outputs with beam quality approximately three times diffraction limited. In addition simple prism tuning has resulted in 0.6-1 wavenumber linewidths throughout the XeCl bandwidth and appears to give an improvement of 50 over short pulse lasers for an equivalent tuning chain.

Embodiment of Concept

The pulse power of the inductively stabilized laser uses discrete doorknob capacitors and a grounded grid thyatron. Figure 1 gives a schematic of the circuit. The loop inductance connecting the main charging capacitance is relatively large as very fast voltage risetimes should no longer be necessary. Because preionization is accomplished via a corona discharge, relatively fast voltage risetimes are still desirable. Since the preionization is weak and only in existence during the rise of the voltage pulse before gas breakdown, it is necessary to bring the current up relatively fast so that the preionization electrons are usable in establishing the initial uniform discharge.

An example of the segmented electrode structures is shown in Fig. 2. There are 87 segments to the electrode. Each segment is ballasted with a 0.15 μ H inductor. The total electrode length is 28 cm with a total active discharge length of 20 cm. Using all five rows of the storage capacitors, the peaking capacitor value is one tenth the storage capacitor value. The peaking capacitor value is nominally 3 nF. The peaking capacitors and the head inductance, plus the stabilizing inductances, establish an approximate tank circuit that rings the voltage and current through the discharge. If the Q of this 28-MHz circuit is high, there will be an additional stabilizing influence to this discharge circuit. However, as will be seen this is not the case and the stabilization of the discharge is mainly accomplished through the influence of the voltage drop across the inductors described earlier.

Parameter Studies

Demonstration of Stabilization. Long pulse lasing is demonstrated in XeCl, XeF, and KrF. Two lasers were constructed having the same length and pulse power circuit. The only difference is that one has a 0.25 cm \times 0.4 cm (electrode separation \times discharge width) and the second has a 1 cm \times 1 cm (electrode separation \times discharge width). The smaller discharge volume device allowed energy deposition greater than 300 J per liter atmosphere without

arcing. The lasing widths in XeCl are compared for the two devices as well as with the lasing pulse width of an earlier miniature laser [3] with unstabilized electrodes and an electrode separation of 0.4 cm. Figure 3 shows a gain in pulse length greater than a factor of 20 over the unstabilized laser. The pulse length and the magnitude of the laser power versus time is dependent on the concentration of the halogen donor and the concentration of the heavier rare gas. Studies of XeCl [4] and KrF [5] were presented previously. We give the parametric behavior in XeF in Fig. 4. The decrease in pulse length with increasing concentrations of fluorine or xenon is attributed to the increasing dynamic resistance of the discharge which, in turn, allows a better match to the impedance of the ringing tank circuit. The result is that more energy is deposited in the earlier phase of the pulse resulting in higher peak power at the beginning of the laser pulse and also shorter laser pulsewidths.

Identification of the Saturation of Energy Deposition. Figure 5 gives the normalized output energy per pulse of XeF, XeCl, and KrF as a function of the stored energy in the main charging capacitors. The main charging capacitors were set up in five rows of twelve 0.5-nF doorknob capacitors each. It is seen from the schematic of Fig. 1 that when only one row or all five rows of capacitors are used the inductance of the primary charging current loop is changed very little. For the 0.25-cm \times 0.4-cm discharge area laser, 70 to 80% of the output energy is obtained with only one row of the charging capacitors even though using all five rows of capacitors, arc free energy deposition over 300 J per liter atmosphere were achieved. The observed saturation of the output energy coupled with the observed saturation in the laser pulse length is disappointing, but at the same time allows a unique opportunity to measure the saturation of energy deposition in rare-gas halide avalanche discharge lasers. Indeed, this saturation of deposited energy is judged to be a "universal" quantity independent of the time scale of the energy deposition. The consequence of such a statement suggests that one must live with high peak power, short pulse lasers or lowered peak power, longer pulse lasers for a given active discharge length, but not both.

Energy Deposition Studies

"Universal" Optimum Energy Deposition Hypothesis. The analysis of the dynamics of the energy deposition requires accurate measurements of voltage and current as a function of time. This is accomplished by incorporating a current probe in the form of a 1/4-inch thick carbon block placed at the bottom electrode as indicated in the schematic given in Fig. 6. Great care is required to place the coaxial probe exactly in the middle of the carbon block to eliminate noise derived from current induced fields. D.C. measurements of the block resistance is not valid as the measured values are dominated by contact resistances which are not present for fast currents. The calibration of this probe is accomplished by first removing the peaking capacitors. The graphite current probe should now see the same current and waveform as the commercial current viewing resistor situated beneath the thyatron as indicated in Fig. 6. Data of energy deposition for one row to five rows of charging capacitors are given in Fig. 7. Voltage, current, power and absolute value of the power are given. The area under the curve of absolute power is the total energy deposited in the first 200 ns of the discharge. The second 200 ns contribute little to the total energy deposition. The deposition of electrical power into the discharge is seen to be in packets and is in agreement with the lasing output shown in Fig. 3. This study is done in the 0.25-cm \times 0.4-cm area laser. The small volume of this discharge (1 cc) means very large energy depositions per liter-atmosphere. The result is that although the power deposition is substantial for over 200 ns, the lasing pulse width is substantially shorter. Figure 8 plots the normalized output lasing energy as a function of the energy density deposited in the first 200 ns of the discharge. Observe that over 300 J per liter-atmosphere of electrical energy have been successfully deposited into the discharge without arcing. However, due to the observed saturation of the output energy this is really not desirable. We measure a saturation energy of 40 J per liter-atmosphere as the optimum deposition energy for highest efficiency. We believe this to be a "universal" number appropriate for XeCl lasers regardless of the time scale of energy deposition.

Test of Hypothesis. If the hypothesis is correct we should increase the discharge volume of the above laser by a factor of 10 so that the deposition energy density will be in the 30 J per liter-atmosphere regime for the case of five rows of charging capacitors. An exact duplicate of the first laser was built and the only change is that the discharge area was enlarged to 1 cm \times 1 cm. Indeed, the observed laser output increased by nearly a factor of 10 to 30 mJ per pulse and the pulse length increased to over 200 ns as shown in Fig. 3.

Measured Electrical Parameters. Figure 7 shows that the discharge head-peaking capacitance section of the circuit sets up a L-C-R tank circuit which rings at a measured period of 36 ns or at a frequency of 28 MHz. Using the equation

$$f_0 = 1/2\pi\sqrt{LC} \quad (1)$$

and a capacitance of $C = 3 \text{ nF}$ an inductance value of 11 nH is obtained. This is a factor of five larger than the inductance of the stabilizing inductance array which is $0.15 \text{ } \mu\text{H}$ (per segment)/87 (segments) = 1.72 nH . Thus, the inductance of the peaking capacitors-discharge head loop is dominated by the head inductance. The resistance R is believed to be dominated by the discharge. The measured impedance is given for the case of five rows of charging capacitors in Fig. 9. The measured impedance for the other storage capacitance values behave similarly. The impedance is seen to oscillate as the voltage crosses zero. The peak value is measured at 0.4 to $0.5 \text{ } \Omega$ and is the discharge resistance. This value is in very good agreement with kinetic code calculations for the dimensions and pressures of the device. If the Q of this tank circuit is high, an added stabilization factor may be playing an important role in these long pulsed excimer laser devices. Using the equation

$$Q = \omega_0 L/R \quad (2)$$

the quality factor for this tank circuit is only $Q = 4$ and should not contribute significantly to the stability of the discharge. Thus, the long pulsed operation of the laser devices described here is primarily due to the stabilization resulting from the individually inductively ballasted electrode segments. The explanation is that as a particular segment begins to streamer arc, the rapid increase in current causes a voltage drop across the inductor and result in a drop in voltage across the discharge gap region. This decrease in voltage across the discharge gap quenches the streamer arc formation. The ringing period of storage capacitance-switch-discharge head loop is over 400 ns . With five rows of capacitors (30 nF) the loop inductance is measured to be 135 nH . As we have stated very little care was taken to lower this inductance. Indeed, this inductance was made quite high to ease the current risetimes in the thyatron switches. It was important to show that under these conditions the stabilization technique can work very effectively delivering long pulsed stable discharge operation in rare gas halide laser mixtures.

Conclusion

The technique of inductive stabilization of rare-gas halide discharges have been shown to yield long pulse laser outputs. The 1% efficiency obtained for the miniature short pulsed devices are believed to be very good. Length scaling to improve the gain per round trip of the laser cavity should improve the peak power in the cavity and greatly improve the extraction efficiency. This work is presently in progress. The measurement of a saturation energy for electrical energy deposition gives an important design criteria for high efficiency lasers. This number is believed to be valid regardless of the time scale of the energy deposition.

Acknowledgements

I wish to acknowledge the expert technical assistance given by Emma Seegmiller. This work is performed under the auspices of the Department of Energy.

References

1. S. Lin and J. Levatter, Appl. Phys. Lett. **34**, 505 (1979); J. Levatter and S. Lin, J. Appl. Phys. **51**, 210 (1980).
2. W. H. Long, M. J. Plummer, and E. A. Stappaerts, Appl. Phys. Lett. **43**, 735-7 (1983).
3. R. C. Sze and E. Seegmiller, IEEE J. Quant. Elec. **QE-17**, 81-91 (1981).
4. R. C. Sze, Proceedings of the Intl' Conference on Lasers '82, 360-4, R. C. Powell, Ed., STS Press (1982).
5. R. C. Sze, Excimer Lasers-1983 (OSA, Lake Tahoe, Nevada), AIP Conference Proceedings No. 100, 73-79, Ed. C. K. Rhodes, H. Egger, and H. Pummer (1983).

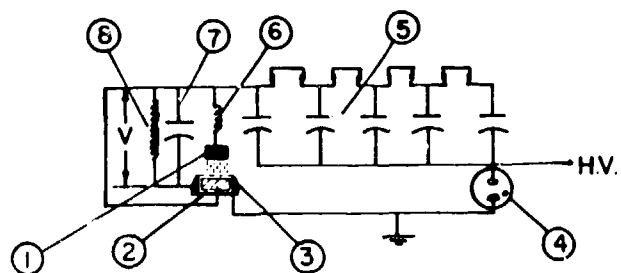


Figure 1. Schematic diagram of inductively stabilized laser. (1) segmented cathodes, (2) corona preionizer, (3) nickel screen anode, (4) thyatron, (5) storage capacitor bank, (6) stabilizing inductors, (7) peaking capacitors, (8) charging inductors.

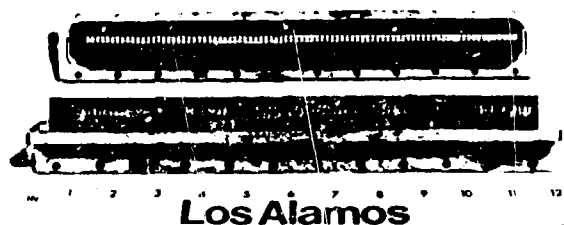


Figure 2. Photograph of 4-mm-wide segmented electrode structure.

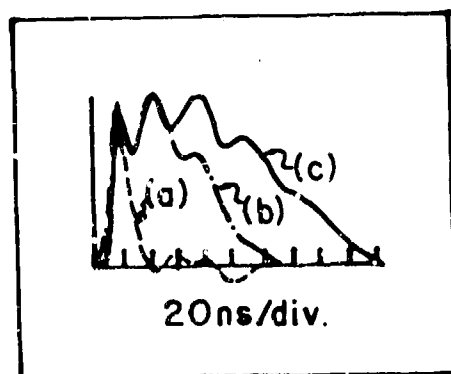


Figure 3. Lasing temporal waveform for (a) unstabilized 4-mm gap separation \times 2-mm-wide laser, (b) stabilized 2.5-mm gap separation \times 4-mm-wide laser, (c) stabilized 10-mm gap separation \times 10-mm-wide laser.

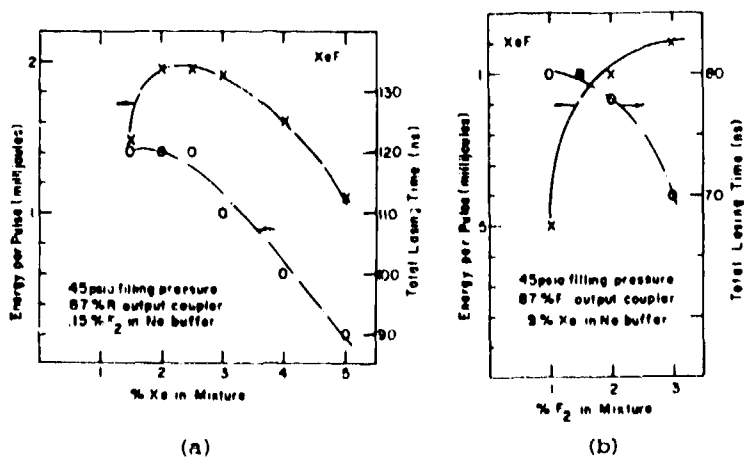


Figure 4. (a) XeF lasing as a function of variations in Xe partial pressure, (b) and F_2 partial pressure.

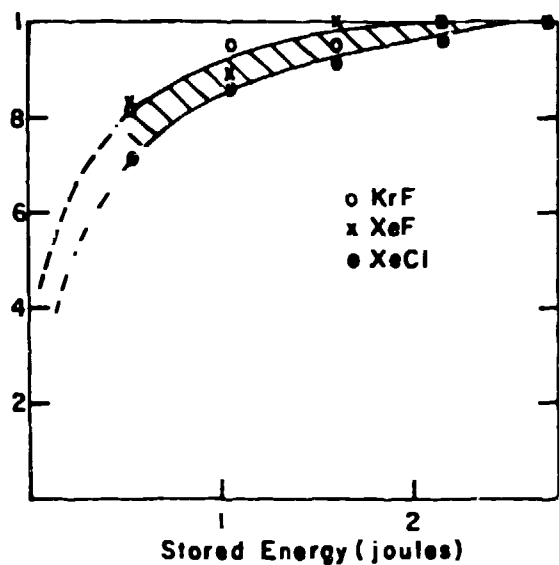


Figure 5. Plot of normalized energy per pulse for XeF (x), XeCl (●), and KrF (o) as a function of stored energy for the 2.5-mm-gap, 4-run-wide inductively stabilized laser.

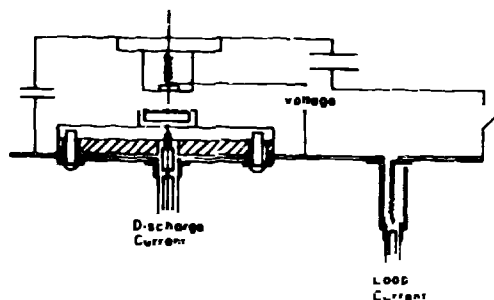
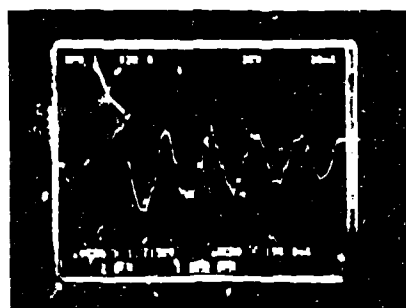
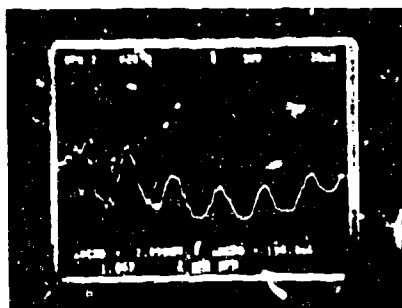


Figure 6. Schematic diagram of experiment to measure energy deposition in the inductively stabilized excimer lasers.



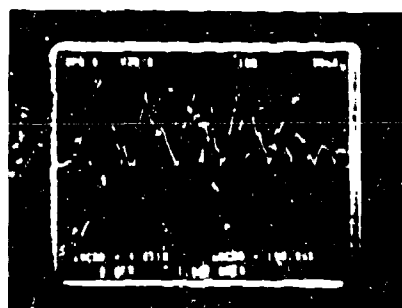
(a)



(b)



(c)



(d)

Figure 7. (a) Voltage, (b) current, (c) power, and (d) absolute value of power waveforms for the case of five rows of charging capacitors (approximately 30 nF at zero charging voltage). Area under curve (d) is the energy deposited into the discharge within the first 200 ns of the discharge.

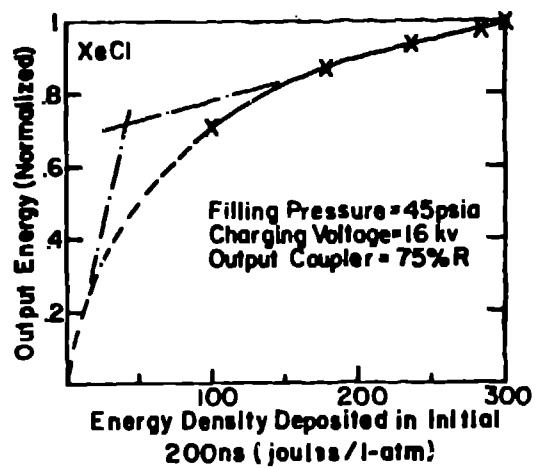
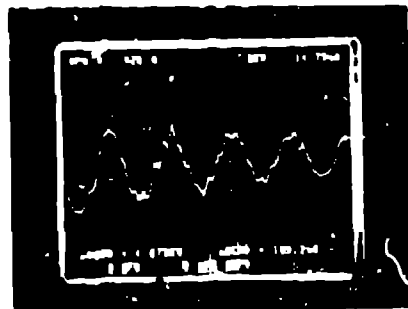
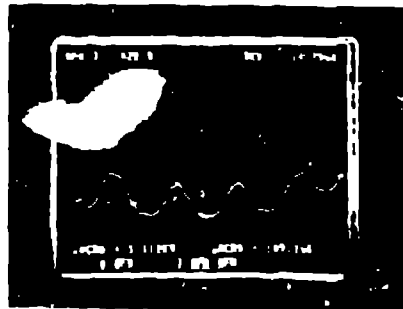


Figure 8. Plot of output energy as a function of energy density deposited in the first 200 ns of the discharge.



(a)



(b)



(c)

Figure 9. Voltage (a), current (b), and impedance - V/I (c), waveforms for the case of five rows of charging capacitors.

END

ATE FILMED

6 / 18 / 84

CONF

PORTIONS OF THIS REPORT ARE ILLEGIBLE. It has been reproduced from the best available copy to permit the broadest possible availability.

Los Alamos National Laboratory is operated by the University of California for the United States Department of Energy under contract W-7405-ENG-38.

CONF-831265-4

LA-UR--84-1190

TITLE:

DE84 011371

INDUCTIVELY STABILIZED EXCIMER LASERS

DISCLAIMER

AUTHOR(S):

Robert C. Sze

This report was prepared as an account of work sponsored by an agency of the United States Government. Neither the United States Government nor any agency thereof, nor any of their employees, makes any warranty, express or implied, or assumes any legal liability or responsibility for the accuracy, completeness, or usefulness of any information, apparatus, product, or process disclosed, or represents that its use would not infringe privately owned rights. Reference herein to any specific commercial product, process, or service by trade name, trademark, manufacturer, or otherwise does not necessarily constitute or imply its endorsement, recommendation, or favoring by the United States Government or any agency thereof. The views and opinions of authors expressed herein do not necessarily state or reflect those of the United States Government or any agency thereof.

SUBMITTED TO:

Proceedings for the International Conference on Lasers 1983
San Francisco, CA, December 1983

MASTER

By acceptance of this article, the publisher recognizes that the U.S. Government retains a nonexclusive, royalty-free license to publish or reproduce the published form of this contribution, or to allow others to do so, for U.S. Government purposes.

The Los Alamos National Laboratory requests that the publisher identify this article as work performed under the auspices of the U.S. Department of Energy

INDUCTIVELY STABILIZED EXCIMER LASERS

Robert C. Sze

Los Alamos National Laboratory

P. O. Box 1663

Los Alamos, New Mexico 87545

anche discharges, including some form of preionization of the discharge to have a limited stable discharge time. The end of the stable discharge is characterized by streamer arcs propagating across the electrodes. This is due to the electrode separation, the constituents and pressure of the gas and the electrical excitation characteristics. Thus, in the more conventional lasers the laser outputs are short pulsed (15-30 ns) and discharge techniques deposit most of the stored electrical energy within the stable discharge. Lin and Levatter [1] have investigated the regimes in which such lasers can be avoided. Such lasers require very uniform preionization with long risetimes. The additional incorporation of an electrical prepulse gives high-efficiency, high-energy large volume discharge rare-gas halide

another approach to solving the problem of discharge stability. The segmented electrode structure with each element ballasted by an inductor gives stable discharges and long pulse length laser outputs. The passive rare-gas halide discharges are attributed mainly to the increase in inductance of a particular segment of the electrode as the discharge becomes unstable. The advantage of the technique is that the very fast current rise is no longer essential, and the use of conventional thyatron current pulse sharpening circuits is now possible. Presently only small lasers are constructed. The 20-cm active length lasers have produced laser pulses less than 200 ns with efficiencies as high as 1%. Since the intracavity gain is low, short gain length devices are in the region of 200 kW, an order of magnitude below the saturation powers of rare-gas halide lasers, much improved extraction is needed for longer gain length devices. The small long pulse lasers are subject to frequency locking large energy short pulsed lasers in the regenerative mode of jitter between the two devices. XeCl, XeF, KrF short pulse lasers are frequency-locked in this manner giving high energy outputs with beam divergence times diffraction limited. In addition simple prism tuning has been demonstrated throughout the XeCl bandwidth and appears to give an alternative to short pulse lasers for an equivalent tuning chain.

The inductively stabilized laser uses discrete doorknob capacitors and inductors. Figure 1 gives a schematic of the circuit. The loop inductance and peaking capacitance is relatively large as very fast voltage risetimes are necessary. Because preionization is accomplished via a corona discharge, long risetimes are still desirable. Since the preionization is weak and the rise of the voltage pulse before gas breakdown, it is necessary that the risetime be relatively fast so that the preionization electrons are usable in the uniform discharge.

The segmented electrode structures is shown in Fig. 2. There are 87 segments. Each segment is ballasted with a 0.15 μH inductor. The total electrode length is a total active discharge length of 20 cm. Using all five rows of the peaking capacitor value is one tenth the storage capacitor value. The value is nominally 3 nF. The peaking capacitors and the head inductors, establish an approximate tank circuit that rings through the discharge. If the Q of this 28-MHz circuit is high, it has a stabilizing influence on this discharge circuit. However, as in the case and the stabilization of the discharge is mainly accomplished by the influence of the voltage drop across the inductors described earlier.

arcing. The lasing widths in XeCl are compared for the two devices as well as with lasing pulse width of an earlier miniature laser [3] with unstabilized electrodes and electrode separation of 0.4 cm. Figure 3 shows a gain in pulse length greater than a factor of 20 over the unstabilized laser. The pulse length and the magnitude of the laser pulse versus time is dependent on the concentration of the halogen donor and the concentration of the heavier rare gas. Studies of XeCl [4] and KrF [5] were presented previously. We show the parametric behavior in XeF in Fig. 4. The decrease in pulse length with increasing concentrations of fluorine or xenon is attributed to the increasing dynamic resistance of the discharge which, in turn, allows a better match to the impedance of the ringing circuit. The result is that more energy is deposited in the earlier phase of the discharge resulting in higher peak power at the beginning of the laser pulse and also shorter pulse widths.

Identification of the Saturation of Energy Deposition. Figure 5 gives the normalized output energy per pulse of XeF, XeCl, and KrF as a function of the stored energy in the charging capacitors. The main charging capacitors were set up in five rows of twelve 0.01-μF doorknob capacitors each. It is seen from the schematic of Fig. 1 that when only one row of capacitors are used the inductance of the primary charging current loop changes very little. For the 0.25-cm × 0.4-cm discharge area laser, 70 to 80% of the output energy is obtained with only one row of the charging capacitors even though using all five rows of capacitors, arc free energy deposition over 300 J per liter atmosphere were achieved. The observed saturation of the output energy coupled with the observed saturation in laser pulse length is disappointing, but at the same time allows a unique opportunity to measure the saturation of energy deposition in rare-gas halide avalanche discharge lasers. Indeed, this saturation of deposited energy is judged to be a "universal" quantity independent of the time scale of the energy deposition. The consequence of such a statement suggests that one must live with high peak power, short pulse lasers or lowered peak power for longer pulse lasers for a given active discharge length, but not both.

Energy Deposition Studies

"Universal" Optimum Energy Deposition Hypothesis. The analysis of the dynamics of energy deposition requires accurate measurements of voltage and current as a function of time. This is accomplished by incorporating a current probe in the form of a 1/4-inch carbon block placed at the bottom electrode as indicated in the schematic given in Fig. 1. Great care is required to place the coaxial probe exactly in the middle of the carbon block to eliminate noise derived from current induced fields. D.C. measurements of the resistance is not valid as the measured values are dominated by contact resistances which are not present for fast currents. The calibration of this probe is accomplished by removing the peaking capacitors. The graphite current probe should now see the same current and waveform as the commercial current viewing resistor situated beneath the thyristor as indicated in Fig. 6. Data of energy deposition for one row to five rows of charging capacitors are given in Fig. 7. Voltage, current, power and absolute value of the power are given. The area under the curve of absolute power is the total energy deposited in the first 200 ns of the discharge. The second 200 ns contribute little to the total energy deposition. The deposition of electrical power into the discharge is seen to be in phase and is in agreement with the lasing output shown in Fig. 3. This study is done in the 0.25-cm × 0.4-cm area laser. The small volume of this discharge (1 cc) means very low energy depositions per liter-atmosphere. The result is that although the power deposition is substantial for over 200 ns, the lasing pulse width is substantially shorter. Figure 8 plots the normalized output lasing energy as a function of the energy density deposited in the first 200 ns of the discharge. Observe that over 300 J per liter-atmosphere of electrical energy have been successfully deposited into the discharge without arcing. However, to the observed saturation of the output energy this is really not desirable. We measure a saturation energy of 40 J per liter-atmosphere as the optimum deposition energy for high efficiency. We believe this to be a "universal" number appropriate for XeCl lasers regardless of the time scale of energy deposition.

Test of Hypothesis. If the hypothesis is correct we should increase the discharge volume of the above laser by a factor of 10 so that the deposition energy density will be in the 30 J per liter-atmosphere regime for the case of five rows of charging capacitors. A duplicate of the first laser was built and the only change is that the discharge area is enlarged to 1 cm × 1 cm. Indeed, the observed laser output increased by nearly a factor of 10 to 30 mJ per pulse and the pulse length increased to over 200 ns as shown in Fig. 9.

Measured Electrical Parameters. Figure 7 shows that the discharge head-peaking capacitance section of the circuit sets up a L-C-R tank circuit which rings at a measured period of 36 ns or at a frequency of 28 MHz. Using the equation

$$f_0 = 1/2\pi\sqrt{LC}$$

(1)

re of $C = 3$ nF an inductance value of 11 nH is obtained. This is a factor of 11 the inductance of the stabilizing inductance array which is $0.15 \mu\text{H}$ (per segments) = 1.72 nH. Thus, the inductance of the peaking capacitors-discharge inductance is dominated by the head inductance. The resistance R is believed to be dominated by the discharge resistance. The measured impedance is given for the case of five rows of charging segments in fig. 9. The measured impedance for the other storage capacitance values begins to oscillate as the voltage crosses zero. The peak impedance is seen at 0.4 to 0.5 Ω and is the discharge resistance. This value is in very good agreement with kinetic code calculations for the dimensions and pressures of the tank circuit is high, an added stabilization factor may be playing a role in these long pulsed excimer laser devices. Using the equation

$$Q = \omega_0 L/R \quad (2)$$

factor for this tank circuit is only $Q = 4$ and should not contribute significantly to the stability of the discharge. Thus, the long pulsed operation of the device described here is primarily due to the stabilization resulting from the inductively ballasted electrode segments. The explanation is that as a partial discharge begins to streamer arc, the rapid increase in current causes a voltage drop across the discharge gap region. This drop in voltage quenches the streamer arc formation. The inductance of storage capacitance-switch-discharge head loop is over 400 ns. With capacitors (30 nF) the loop inductance is measured to be 135 nH. As we have taken the care was taken to lower this inductance. Indeed, this inductance was reduced to ease the current risetimes in the thyatron switches. It was important under these conditions the stabilization technique can work very effectively for long pulsed stable discharge operation in rare gas halide laser mixtures.

Results of inductive stabilization of rare-gas halide discharges have been shown for long pulse laser outputs. The 1% efficiency obtained for the miniature short pulse laser are believed to be very good. Length scaling to improve the gain per round trip in the cavity should improve the peak power in the cavity and greatly improve the efficiency. This work is presently in progress. The measurement of a figure of merit for electrical energy deposition gives an important design criteria for excimer lasers. This number is believed to be valid regardless of the time scale or position.

We acknowledge the expert technical assistance given by Emma Seegmiller. This work was done under the auspices of the Department of Energy.

J. Levatter, Appl. Phys. Lett. 34, 505 (1979); J. Levatter and S. Lin, J. Appl. Phys. 51, 210 (1980).

M. J. Plummer, and E. A. Stappaerts, Appl. Phys. Lett. 43, 735-7 (1983).

and E. Seegmiller, IEEE J. Quant. Elec. QE-17, 81-91 (1981).

Proceedings of the Intl' Conference on Lasers '82, 360-4, R. C. Powell, Ed. (1982).

Excimer Lasers-1983 (OSA, Lake Tahoe, Nevada), AIP Conference Proceedings 79, Ed. C. K. Rhodes, H. Egger, and H. Plummer (1983).

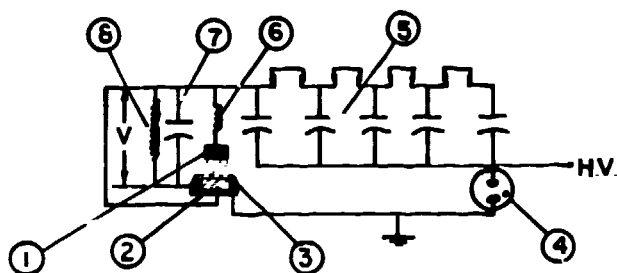


Figure 1. Schematic diagram of inductively stabilized laser. (1) segmented cathodes, (2) corona preionizer, (3) nickel screen anode, (4) thyatron, (5) storage capacitor bank, (6) stabilizing inductors, (7) peaking capacitors, (8) charging inductors.

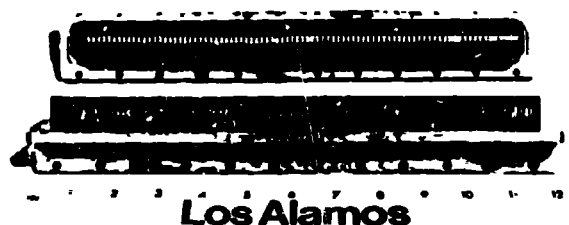


Figure 2. Photograph of 4-mm-wide segmented electrode structure.

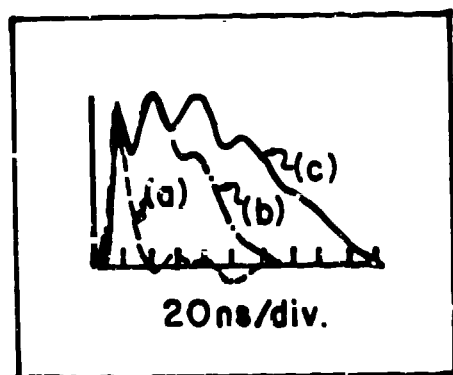


Figure 3. Lasing temporal waveform for (a) unstabilized 4-mm gap separation \times 2-mm-wide laser, (b) stabilized 2.5-mm gap separation \times 4-mm-wide laser, (c) stabilized 10-mm gap separation \times 10-mm-wide laser.

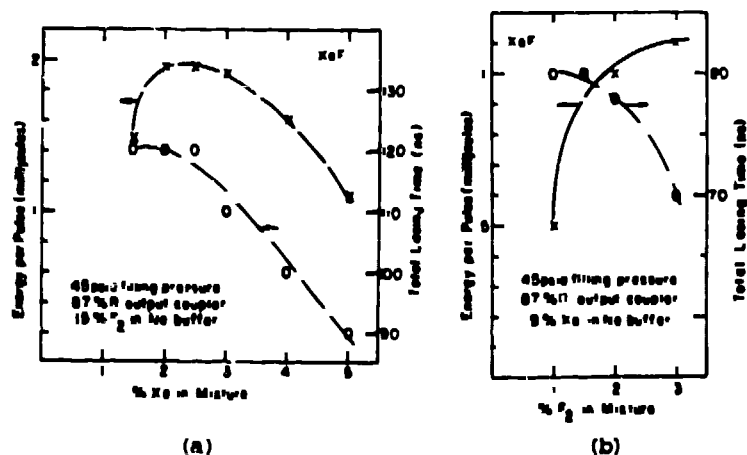
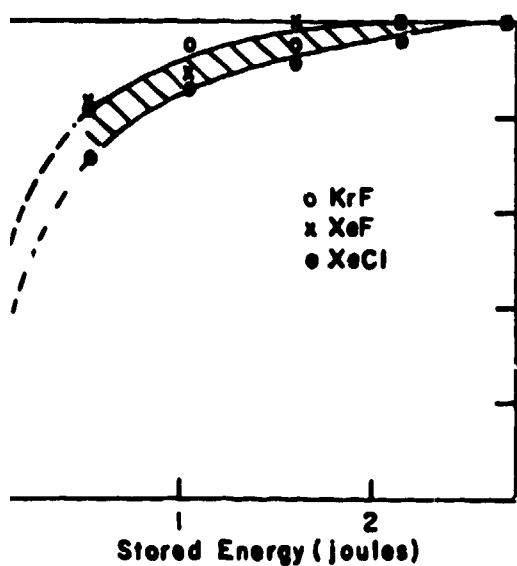


Figure 4. (a) XeF lasing as a function of variations in Xe partial pressure, (b) and F_2 partial pressure.



5. Plot of normalized energy per pulse $F(x)$, XeCl (●), and KrF (○) as a function of stored energy for the 2.5-mm-gap tion \times 4-mm-wide inductively stabilized

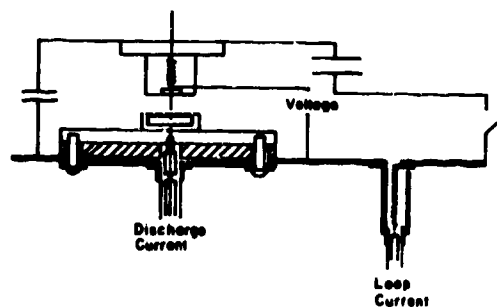
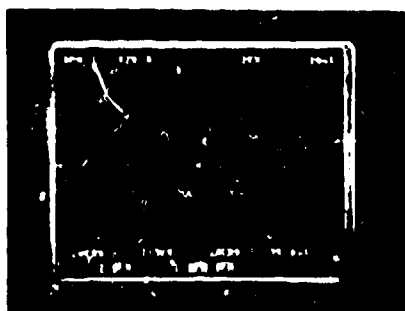


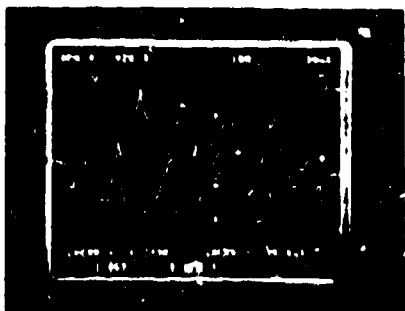
Figure 6. Schematic diagram of experiment to measure energy deposition in the inductively stabilized excimer lasers.



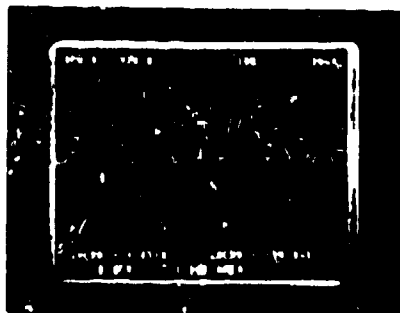
(a)



(b)



(c)



(d)

Figure 7. (a) Voltage, (b) current, (c) power, and (d) absolute value of power

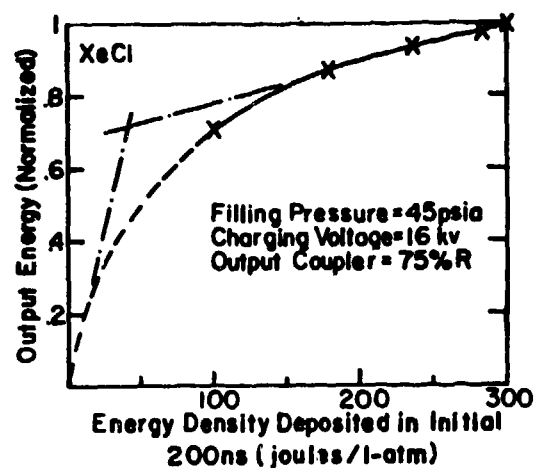
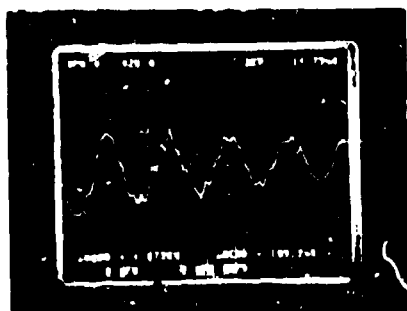
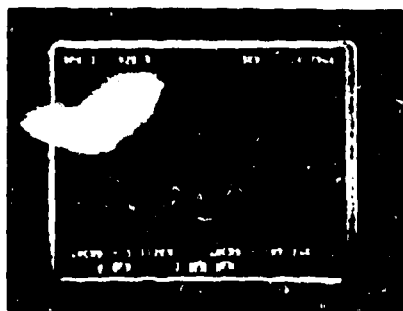


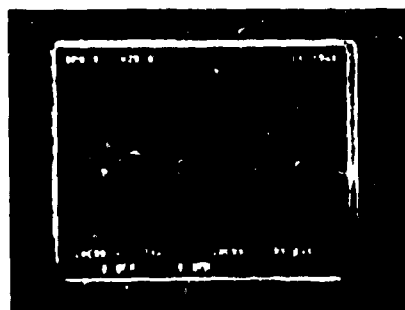
Figure 8. Plot of output energy as a function of energy density deposited in the first 200 ns of the discharge.



(a)



(b)



(c)